

Fabrication of Ultra-High Q Silica Microdisk Using Chemo-Mechanical Polishing

S. Honari,¹ S. Haque,¹ and T.Lu^{1, a)}

*Electrical and Computer Engineering Department, University of Victoria,
EOW 448, 3800 Finnerty Rd., Victoria, BC V8P 5C2, Canada*

(Dated: 13 April 2021)

Here we demonstrate that adding a chemo-mechanical polishing (CMP) procedure to conventional photolithography, a silica microdisk with ultra-high quality factors ($> 10^8$) can be fabricated. By comparing with the intrinsic optical quality factor (Q) measured at 970 nm, we observe that due to the significantly reduced surface roughness, at 1550 nm wavelength the water molecule absorption at the cavity surface supersedes Rayleigh scattering as the dominant factor for Q degradation.

The study of whispering gallery mode (WGM) micro resonators has dominated many fields of science over past decades. Microcavities have become one of the most attractive optical components to study in a broad range of scientific disciplines, including but not limited to, nanoparticle detection, biosensing, quantum information, comb generation, and optomechanics¹⁻⁶. The power of microcavities to confine the light is mostly measured by optical quality factor (Q) as the higher the Q goes the more intense the light inside the cavity becomes.⁷ High Q microcavities are essential for better detection in sensing applications, lower threshold power for comb generation, and parametric oscillation^{8,9} and narrower linewidth for laser oscillators.¹⁰

One of the most important limiting factors for achieving high Q is Rayleigh scattering induced by surface roughness¹¹. Hence, efforts to increase the optical Q has mainly relied on using the expensive fabrication techniques such as stepper lithography¹² or CO₂ laser reflow¹³ to decrease the surface roughness of microcavities and increase the Q. However, these techniques come with either the need for expensive machinery or incompatibility with monolithic integration. Silica microdisks with Q exceeding 1 billion have been fabricated recently by carving out the Silica and making trenches on grown silica film rather than making stand alone disks.¹⁴ High Q microresonators and low loss waveguides from other nonlinear materials have also been demonstrated with deposition on silica platforms to take advantage of smooth surface and low loss nature of the oxide.¹⁵

Chemo-mechanical polishing (CMP) has been used to increase the optical Q for LiNbO₃^{16,17} and Si₃N₄¹⁸ microdisks, but to the best of our knowledge, this technique has not been used to fabricate SiO₂ microdisks. In this paper we incorporate CMP to conventional photolithography to fabricate ultra-high Q microdisks. Through scanning electron microscopy (SEM) and numerical modelling, we further analyze limiting factors to further Q improvement.

Our fabrication process consists of four steps: a) conventional photolithography using deep UV light, b) wet etching of SiO₂ using buffered HF, c) chemomechanical polishing of the SiO₂ disks with silica slurry, and d) XeF₂ dry etch of the Silicon layer to form the pillars (Fig 1).

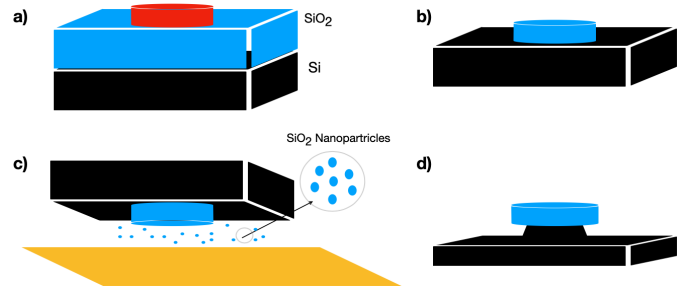


FIG. 1. a) Photolithography of the resist to transfer the pattern, b) HF wet etch to make the disk, c) CMP step to increase the smoothness of the surface, and d) etching Si substrate to make the pillar.

The fabrication details are as follows. After applying a standard wafer cleaning process, we spin coat a silica-on-silicon wafer (SoS, University Wafers) with positive resist (S1813). A UV lithography is then applied to transfer the microdisk pattern from the photomask onto the wafer followed by a buffered HF (Transene) wet etch to form disks on the silica thin film. To further improve the surface smoothness of the disks, we proceed to the polishing step using slurry of 70-nm-diameter silica nanoparticles. Before the polishing step can be done, it is important to change the surface chemistry of the sample. Hydrogen passivation surface of the sample after HF wet etching makes the surface extremely hydrophobic,¹⁹ which can hinder the flow of slurry and reduce the effectiveness of the CMP step significantly. In order to remedy this problem, we used a 10 minutes Piranha solution (H₂SO₄/H₂O₂) to clean the surface and make it hydrophilic. Hand polishing of the sample was then performed using the silica nanoparticle slurry to reduce the surface roughness. RCA cleaning steps has also been performed after polishing to wash off the slurry particles stick to the surface of the disk. In the last step of fabrication, XeF₂ gas was used inside an etching chamber to undercut the disk and form the pillars by etching the silicon underneath the disks. This step is crucial for achieving high Q micro resonators, since the light silicon interaction inside the cavity should be minimized. The maximum amount of undercut is limited by the buckling effect that happens at larger undercuts, and can degrade the Q or even make the disk crack. However, the problem can be mitigated by high temperature annealing (1,000 °C).¹⁴

^{a)}Electronic mail: taolu@ece.uvic.ca

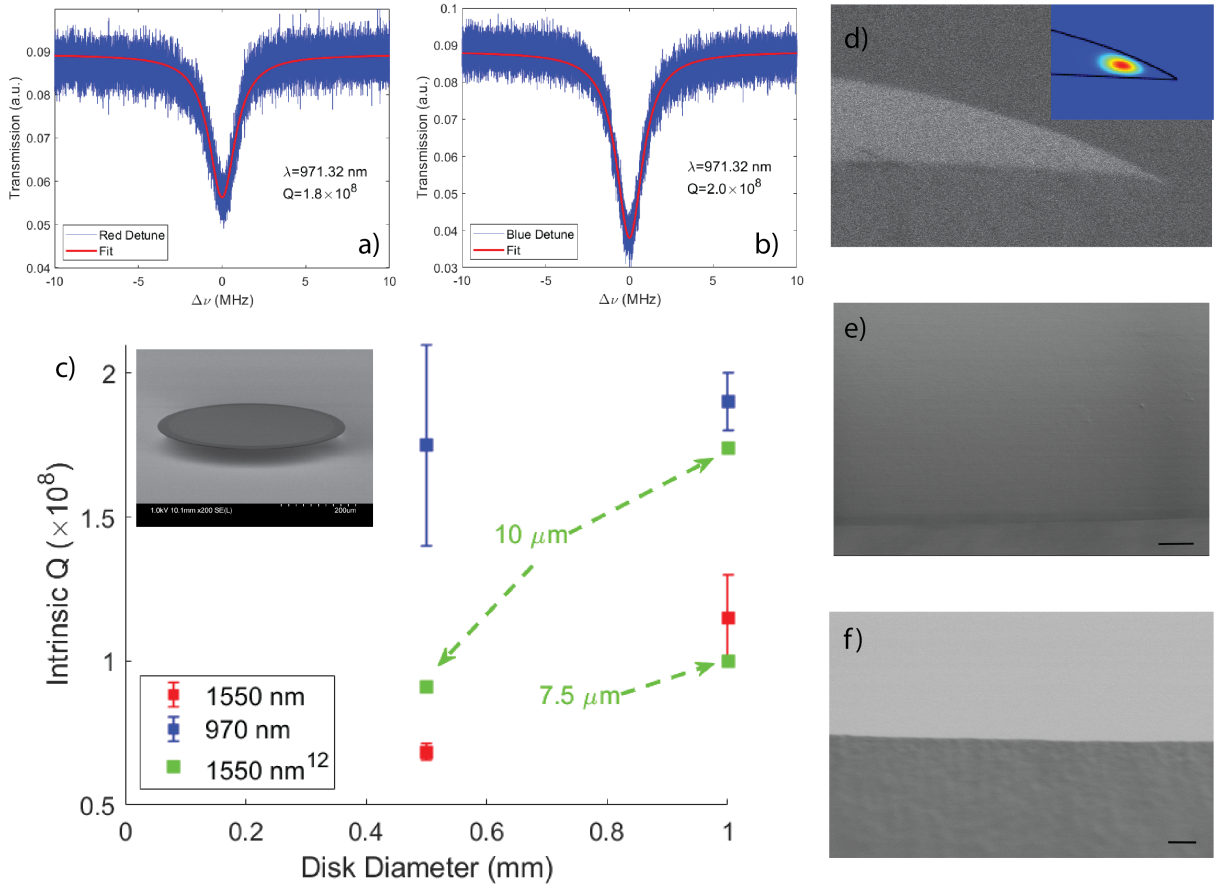


FIG. 2. Transmission spectra of a 1 mm disk when the 970 nm probe laser wavelengths scanned toward a) red (blue traces) and b) blue detune (blue trace). The intrinsic Qs of 1.8×10^8 and 2.0×10^8 were obtained through least square fitting to a Lorentzian function (red traces) respectively, indicating the intrinsic Q to be $(1.9 \pm 0.1) \times 10^8$. c) Intrinsic Q as a function of disk diameter at 970 nm (blue squares), 1550 nm (red squares) wavelength bands with the lengths of the error bars corresponding to the differences of the measured intrinsic Q at red and blue detune. In comparison, the recorded values of 7.5 μm and 10 μm thick microdisks by Lee et. al.¹² are displayed as green squares. Note that, after polishing, the silica thin film thickness of our disks reduced from 10 μm to 7.5 μm . d) The side view SEM micrograph of a polished disk at its edge shows the side wall vanishes after polishing. e) the topview micrograph further confirms the sharp corner at the edge of the upper surface were polished away as oppose to the unpolished disk displayed in f). The comparison also demonstrates the reduced surface roughness through CMP.

In the next step, we measure the intrinsic Qs at 970 nm and 1550 nm wavelength bands. Here, external cavity tunable lasers (Samtec TSL-550 for 1550 nm, and Newfocus TLB 6718-D for 970 nm) were used to probe the microdisks through a tapered optical fiber. As shown in Fig. 2a, by linearly scanning the laser around the cavity resonance wavelength, a Lorentzian shaped signal will appear at the output transmission of the tapered fiber, from which intrinsic Q can be calculated. Here, to accurately readout the optical frequency, we placed a fiber Mach-Zehnder interferometer in parallel to the microdisk cavity as a reference.² Note that, the intrinsic Q values measured by red detuning and blue detuning of the laser wavelengths are slightly different, due to the thermal effects. Therefore, we take the average of both Qs as the estimated value of intrinsic Q and their difference as the uncertainty. For example, as shown on Fig. 2a, the Q measured from blue detuning on a 10 μm (7.5 μm after polishing) thick, 1mm diameter microdisk using a 970 nm laser was 2.0×10^8

while Fig. 2b shows that from a red detuned measurement the Q of 1.8×10^8 was obtained. Consequently we determine the intrinsic Q to be $(1.9 \pm 0.1) \times 10^8$ as shown in Fig. 2c (blue square with error bars representing the uncertainty). We also used our fabrication process to make 500 μm disks, and the average intrinsic Q of $(1.8 \pm 0.4) \times 10^8$ was obtained. In order to better compare our work with previously reported results (green squares),¹² we used 1550 nm laser to measure the Q as well. We observed the optical Q drops to $(1.2 \pm 0.2) \times 10^8$ for 1 mm disk and $(6.9 \pm 0.2) \times 10^7$ for 500 μm disk (red squares in Fig. 2b). Note that the Q of our 1 mm disk is slightly better than the equivalent 7.5 μm thick disks reported in.¹² The side view and top view SEM micrographs in Fig. 2d-e show reduced roughness on the polished surface compared to the unpolished one shown in Fig. 2f and confirms our process make the disk edges more smooth, which will reduce the Rayleigh scattering. The edge shape has altered after the CMP step and the sharp angle between the top surface and the sidewall

has changed to a smooth gradual change in angle, so that top surface and the sidewall are almost indistinguishable. This change in turn would affect the mode position inside the cavity as shown in the inset of Fig. 2d.

Further, the observation of lower Q at longer wavelength suggests Rayleigh scattering is not the dominant factor for Q degradation. Instead, water absorption at the disk surface dominates the Q at 1550 nm since otherwise surface roughness induced Rayleigh scattering should make the Q at shorter wavelength (970 nm) even lower.²⁰ This contradicts the previous observations that Q at 1550 nm is limited by surface roughness.^{21–23} To confirm, we numerically simulate the modes and compare the intrinsic Q at both wavelengths. In simulation, the side view SEM image of the disk in Fig. 2d was converted to a contour curve for COMSOL simulation as shown on its inset (black trace). In the absence of water layer, the Q of 2.12×10^{10} at 970 nm and 2.69×10^{10} at 1550 nm were obtained through simulations. Since our SEM does not provide sufficient resolution for surface roughness, the simulated Q were mainly silica material absorption limited. We then added a layer of water at the disk surface and obtained a Q of 1.56×10^8 at 1550 nm when the water layer is 1 nm thick. This is in close agreement to our experiment observation around this wavelength. On the other hand, the simulated Q at 970 nm was 4.14×10^9 due to the significantly lower water absorption at this wavelength band. As the experimental measurement ($Q = (1.9 \pm 0.1) \times 10^8$) is much lower than the simulation value, we confirm that at 970 nm Q is still limited by Rayleigh scattering. In fact, assuming the Rayleigh scattering induced Q (Q_{ss}) has λ^3 dependence²⁰ and $Q_{ss} \sim 1.9 \times 10^8$ at 970 nm, one would expect $Q_{ss} \sim 7.8 \times 10^8$ at 1550 nm, which is much higher than the measured Q . From these observations, we concluded that at 1550 nm, Q is limited by a 1-nm water layer absorption while at 970 nm surface roughness is still the limiting factor for Q .

In summary, we made microdisks with ultra high optical Q using conventional photolithography in conjunction with CMP. As a result, surface roughness is no longer a limiting factor for Q at 1550 nm. The Q at shorter wavelength can be further improved by using smaller nanoparticles as slurry to achieve lower surface roughness. Through simulation, we further find that by removing the 1 nm water layer at the microdisk surface, a Q value close to 10^9 can be reached at 1550 nm.

This work was supported in part by the Nature Science and Engineering Research Council of Canada (NSERC) Discovery (Grant No. RGPIN-2020-05938), and Threat Reduction Agency (DTRA) Thrust Area 7, Topic G18 (Grant No. GRANT12500317). We would like to acknowledge CMC Microsystems for the provision of products and services that facilitated this research, including the use of COMSOL for the numerical analysis. The authors would like to thank Dr. Elaine Humphrey, Mr. Jon Rudge, and the staff of Advanced Microscopy Facility (AMF) at University of Victoria for their help and constructive and valuable discussions. The data that support the findings of this study are available from the corresponding author upon reasonable request.

- ¹K. J. Vahala, "Optical microcavities," *Nature* **424**, 839–846 (2003).
- ²T. Lu, H. Lee, T. Chen, S. Herchak, J.-H. Kim, S. E. Fraser, R. C. Flagan, and K. Vahala, "High sensitivity nanoparticle detection using optical microcavities," *Proceedings of the National Academy of Sciences* **108**, 5976–5979 (2011).
- ³M. D. Baaske, M. R. Foreman, and F. Vollmer, "Single-molecule nucleic acid interactions monitored on a label-free microcavity biosensor platform," *Nature Nanotechnology* **9**, 933 (2014).
- ⁴T. J. Kippenberg, R. Holzwarth, and S. A. Diddams, "Microresonator-based optical frequency combs," *Science* **332**, 555–559 (2011).
- ⁵S. B. Papp, K. Beha, P. Del'Haye, F. Quinlan, H. Lee, K. J. Vahala, and S. A. Diddams, "Microresonator frequency comb optical clock," *Optica* **1**, 10–14 (2014).
- ⁶T. J. Kippenberg and K. J. Vahala, "Cavity optomechanics: back-action at the mesoscale," *Science* **321**, 1172–1176 (2008).
- ⁷A. Campillo, J. Eversole, and H. Lin, "Cavity quantum electrodynamic enhancement of stimulated emission in microdroplets," *Physical Review Letters* **67**, 437 (1991).
- ⁸T. Kippenberg, S. Spillane, and K. Vahala, "Kerr-nonlinearity optical parametric oscillation in an ultrahigh-Q toroid microcavity," *Physical Review Letters* **93**, 083904 (2004).
- ⁹V. S. Ilchenko, A. A. Savchenkov, A. B. Matsko, and L. Maleki, "Nonlinear optics and crystalline whispering gallery mode cavities," *Physical Review Letters* **92**, 043903 (2004).
- ¹⁰J. Li, H. Lee, T. Chen, and K. J. Vahala, "Characterization of a high coherence, Brillouin microcavity laser on silicon," *Optics Express* **20**, 20170–20180 (2012).
- ¹¹M. L. Gorodetsky, A. D. Pryamikov, and V. S. Ilchenko, "Rayleigh scattering in high-Q microspheres," *JOSA B* **17**, 1051–1057 (2000).
- ¹²H. Lee, T. Chen, J. Li, K. Y. Yang, S. Jeon, O. Painter, and K. J. Vahala, "Chemically etched ultrahigh-Q wedge-resonator on a silicon chip," *Nature Photonics* **6**, 369–373 (2012).
- ¹³D. Armani, T. Kippenberg, S. Spillane, and K. Vahala, "Ultra-high-Q toroid microcavity on a chip," *Nature* **421**, 925–928 (2003).
- ¹⁴L. Wu, H. Wang, Q. Yang, Q.-x. Ji, B. Shen, C. Bao, M. Gao, and K. Vahala, "Greater than one billion Q factor for on-chip microresonators," *Optics Letters* **45**, 5129–5131 (2020).
- ¹⁵D.-G. Kim, S. Han, J. Hwang, I. H. Do, D. Jeong, J.-H. Lim, Y.-H. Lee, M. Choi, Y.-H. Lee, D.-Y. Choi, *et al.*, "Universal light-guiding geometry for on-chip resonators having extremely high Q-factor," *Nature Communications* **11**, 1–7 (2020).
- ¹⁶R. Wu, J. Zhang, N. Yao, W. Fang, L. Qiao, Z. Chai, J. Lin, and Y. Cheng, "Lithium niobate micro-disk resonators of quality factors above 10^7 ," **43**, 4116–4119.
- ¹⁷M. Wang, R. Wu, J. Lin, J. Zhang, Z. Fang, Z. Chai, and Y. Cheng, "Chemo-mechanical polish lithography: A pathway to low loss large-scale photonic integration on lithium niobate on insulator," *Quantum Engineering* **1**, e9 (2019).
- ¹⁸X. Ji, F. A. Barbosa, S. P. Roberts, A. Dutt, J. Cardenas, Y. Okawachi, A. Bryant, A. L. Gaeta, and M. Lipson, "Ultra-low-loss on-chip resonators with sub-milliwatt parametric oscillation threshold," *Optica* **4**, 619–624 (2017).
- ¹⁹G. Trucks, K. Raghavachari, G. Higashi, and Y. Chabal, "Mechanism of HF etching of silicon surfaces: A theoretical understanding of hydrogen passivation," *Physical Review Letters* **65**, 504 (1990).
- ²⁰M. Borselli, K. Srinivasan, P. E. Barclay, and O. Painter, "Rayleigh scattering, mode coupling, and optical loss in silicon microdisks," *Applied Physics Letters* **85**, 3693–3695 (2004).
- ²¹D. Vernooy, V. S. Ilchenko, H. Mabuchi, E. Streed, and H. Kimble, "High-Q measurements of fused-silica microspheres in the near infrared," *Optics Letters* **23**, 247–249 (1998).
- ²²H. Rokhsari, S. Spillane, and K. Vahala, "Loss characterization in microcavities using the thermal bistability effect," *Applied Physics Letters* **85**, 3029–3031 (2004).
- ²³D. Ganta, E. Dale, and A. Rosenberger, "Measuring sub-nm adsorbed water layer thickness and desorption rate using a fused-silica whispering-gallery microresonator," *Measurement Science and Technology* **25**, 055206 (2014).